A general algorithm for building 3D spatial laws from lower dimensional structural information

Jef Caers
Stanford University

Introduction

In geostatistics or spatial statistics, stochastic simulation aims at building multiple three-dimensional models, each representing possible alternative representations or realizations of the spatial variability of an actual true field under study. These models generally carry two important properties: (1) they match some local or global data and (2) they reflect the believed spatial variability of the variable under investigation. This paper will focus on the latter.

We consider the modeling of a spatial variable of certain support on a grid, either regular or irregular. In modeling such variables, the random function concept is used, which is fully characterized by its spatial law, defining the joint probability in terms of a probability mass function (pmf) for a discrete variable

$$P(a_1, a_2, a_3, \ldots, a_N) = \Pr(A_1 = a_1, A_2 = a_2, A_1 = a_3, \ldots, A_N = a_N) \qquad (1)$$

where A_i is a discrete random variable at location i with outcome a_i, or, in the continuous case, the joint cumulative distribution function (cdf),

$$F(z_1, z_2, z_3, \ldots, z_N) = \Pr(Z_1 \le z_1, Z_2 \le z_2, Z_3 \le z_3, \ldots, Z_N \le z_N)$$

The approach advocated in statistical circles consists of defining these joint distributions analytically or at least somewhat explicitly, then estimate the distribution parameters from data, finally, sample realizations using either direct or iterative sampling procedures. For this purpose, in the continuous case, one spatial law is particularly convenient and fully analytically known, namely the multi-Gaussian law. The multi-Gaussian pdf after normal score transform is fully defined by its first two moments, mean **m** and covariance matrix C:

$$f(y_1, y_2, y_3, \ldots, y_N, \mathbf{m}, C) = \frac{1}{(2\pi)^{\frac{3}{2}} \det(C)} \exp\left(-\frac{1}{2} (\mathbf{y} - \mathbf{m})^T C^{-1} (\mathbf{y} - \mathbf{m}) \right)$$

where Y_i is a normal score transform of variable Z_i. Sampling from this law can be done without approximation either through LU decomposition or through eigenvalue decomposition of the covariance matrix C. Since this is prohibitive on large 3D grid,

good approximations exist through sequential simulation or iterative McMC sampling. In such approximation, the actual spatial law sampled depends additionally on the particular algorithmic implementation, usually requiring the definition of certain tuning parameters $\boldsymbol{\theta}$ (e.g. search neighborhood in sequential simulation or stopping criterion in iterative sampling). Hence, the actual spatial law sampled is not multi-Gaussian, only an approximation thereof:

$$f(y_1, y_2, y_3, \ldots, y_N, \mathbf{m}, C, \boldsymbol{\theta}) \approx f(y_1, y_2, y_3, \ldots, y_N, \mathbf{m}, C) \qquad (2)$$

From a practical point of view this is not a major problem, since the limited data never allows one to check or test if the multi-Gaussian really applies. The multi-Gaussian framework is only useful in the sense that it ensures reproduction of the spatial covariance C, which in the best case can be statistically inferred from data. Moreover, real spatial data are never univariate Gaussian, let alone multi-Gaussian. If such data is used as conditioning information, then the resulting conditional spatial law

$$f(y_1, y_2, y_3, \ldots, y_N, \mathbf{m}, C \mid \text{local data})$$

will not be multi-Gaussian even if exact algorithms were applied. However, the problem with the multi-Gaussian law does not lie so much in the approximation given by (2), it lies in the fact that the resulting realizations do no reflect any realistic spatial variability mimicking that observed in nature. Consider the reason why: choosing a multi-Gaussian law results in all higher moments being uniquely defined by the spatial covariance C. There exist many different consistent sets of higher moments that share a similar spatial covariance. The multi-Gaussian model provides one such consistent set, but its realizations have minimal structure[1] beyond the given spatial covariance (maximum entropy property).

As a solution, a new field in spatial modeling has been recently introduced, termed multiple-point statistics. While a minimal amount of statistical/structural[1] information is required in a multi-Gaussian framework (mean and covariance only), the mp-geostatistical approach lies near the other spectrum, requiring one to provide most higher-order statistics explicitly. The latter are inferred explicitly or implicitly through a training image. A training image is a fully explicit 3D realization of the believed spatial variability. It can be regarded as a database from which several higher order or multi-point statistics can be extracted. To define spatial laws based on a training image two approaches exists.

The first approach relies on the explicit definition of a spatial law, termed Markov random field. A Markov random field is defined by a fully explicit (up to normalization constant) parametric pmf as a model for (1). Any conditional pmf is thus explicitly known up to a normalization constant. The parameters can be estimated from the training

[1] The word "structural" does not refer to a fault or horizon structure. It is geostatistical jargon for any prior statistical information, such as a variogram, describing the spatial variability of the field of study.

image statistics, and realizations are drawn using McMC simulation. Both parameter inference and sampling can be tedious and CPU demanding.

The second approach does not rely on a prior definition of a parametric joint or conditional pmf. Instead, an algorithmic approach is taken by means of sequential simulation. Any sequential simulation calls for the modeling of the conditional distribution of a variable A_i given all previously simulated variables. Such conditional distributions/statistics can be directly scanned from the training image, no prior modeling need to take place. In case conditional statistics are not present in the training image, the number if conditioning data is reduced, e.g. previously simulated values are omitted, until inference from the training image is possible. For this reason, one requires training images to be as large as possible, containing a rich and varied set of higher order statistics.

The Achilles' heal of this approach lies in the prerequisite to have available a 3D training image, which may be impossible in many practical applications. Hence, the multi-point statistical approach is often dropped for a traditional two-point (spatial covariance approach). Currently, one has to decide between these two extremes. In many Earth Science applications, particularly in subsurface modeling, structural information comes only in parts, such as along a vertical direction (from wells), along a vertical cross section such as from analog outcrops, or, along a horizontal plane such as from seismic on shallower analogs or from aerial photos. In space-time modeling a similar situation arises: structural information comes from a well-informed time-component and a well-informed spatial component, a fully 4D (space-time) training image would be difficult to create. The problem of constructing full 3D/4D spatial laws when only partial and lower-dimensional structural information is available is tackled in this paper.

Methodology

From joint to conditionals

Consider for reasons of presentation only the case of a binary spatial variable A, which has outcome '1' or '0'. The proposed method relies on the following sequential decomposition of a joint pmf of the type (1)

$$\Pr(A_1 = a_1, A_2 = a_2, A_1 = a_3, \ldots, A_N = a_N) = \Pr(A_1 = a_1) \times \Pr(A_2 = a_2 \mid a_1) \times \ldots \times \Pr(A_N = a_n \mid a_{n-1}, \ldots a_1) \quad (3a)$$

This decomposition is exact. The spatial law is fully defined, if each conditional pmf is fully defined. Each conditional pmf is denoted as,

$$\Pr(A_j = a_j \mid a_{j-1}, a_{j-2}, \ldots a_1) = \Pr(A_j = a_j \mid (j-1)) \quad (3b)$$

In a spatial covariance approach one relies on the joint statistical modeling of all two-point conditionals $Pr(A_j|A_i)$ through indicator variograms, then use this partial information to define the full conditional probability of the type (3b) through indicator kriging.

$$Pr^*(A_j = a_j \mid a_{j-1}, a_{j-2}, \ldots a_1) - Pr(A_j = a_j) = \sum_{i=1}^{j-1} \lambda_\alpha \left(a_i - Pr(A_i = a_i)\right)$$

The * indicated that this is a model/estimate for (3b). Indicator kriging calls for the indicator covariance between any two events A_i and A_j, which is equivalent to calling for the conditionals $Pr(A_j|A_i)$. Indeed, consider the dual indicator kriging expression

$$\begin{aligned} &Pr^*(A_j = 1 \mid a_{j-1}, a_{j-2}, \ldots a_1) - Pr(A_j = 1) = \sum_{i=1}^{j-1} d_i Cov(A_j, A_i) \\ &\text{where } Cov(A_j, A_i) = Pr(A_i = 1) \times \left(Pr(A_j = 1 \mid A_i = 1) - Pr(A_j = 1)\right) \end{aligned} \qquad (4)$$

The indicator kriging takes into account the redundancy of information between any two data A_i and A_k on determining A_j. The dual kriging weights d_i can be seen as weights given to each partial conditional $Pr(A_j|A_i)$. Since the probability in (4) is modeled through covariance functions, restrictions need to be set on these functions to make the probabilities licit. This often leads to a tedious fitting exercise.

In a multiple-point approach, the probability of type (3b) is directly inferred from the training image, no tedious modeling of covariance functions is required. This is achieved by considering Bayes' rule

$$\begin{aligned} Pr(A_j = a_j \mid a_{j-1}, a_{j-2}, \ldots a_1) &= \frac{P(a_j, a_{j-1}, a_{j-2}, \ldots, a_1)}{P(a_{j-1}, a_{j-2}, \ldots, a_1)} \\ &\approx \frac{\#\text{ events } \{a_j, a_{j-1}, a_{j-2}, \ldots, a_1\}}{\#\text{events } \{a_j = 0, a_{j-1}, a_{j-2}, \ldots, a_1\} + \#\text{events } \{a_j = 1, a_{j-1}, a_{j-2}, \ldots, a_1\}} \end{aligned}$$

where the # events $\{a_j=0,a_{j-1},a_{j-2},\ldots a_1\}$ and # events $\{a_j=1,a_{j-1},a_{j-2},\ldots a_1\}$ can be obtained directly by scanning the training image for replicates of $\{a_{j-1},a_{j-2},\ldots a_1\}$ and counting the number of times $\{a_j=1\}$ occurs. In cases when the conditioning event $\{a_{j-1},a_{j-2},\ldots a_1\}$ cannot be found in the training image, then, a selected set of values a_k are dropped from $\{a_{j-1},a_{j-2},\ldots a_1\}$ until enough replicates are found in the training image. The implicit assumption made is that the values a_k dropped are conditionally independent of a_j given the remaining a_i.

Modeling with partial information

The multiple-point approach requires one to have information on the frequency of the full 3D conditioned event $\{a_j \mid a_{j-1},a_{j-2},\ldots a_1\}$, which may not be available in practice. Instead, one may have partial information in the form of a set of M probabilities

$$\Pr(A_j = a_j \mid \{a\}_m), \quad m = 1,\ldots,M$$

where $\{a\}_m$ denotes any subset of the conditioning event $(j-1)=\{a_j,a_{j-1},a_{j-2},\ldots a_1\}$. We assume that M $\Pr(A_j=a_j \mid \{a\}_m)$ such probabilities are available. In other word M different sources of partial spatial continuity data are available. The union of all $\{a\}_m$ need not equal (j-1), which means that the total sum of all partial information may not provide a full and unique 3D quantification of spatial variability. Also, some conditioning values a_k may be shared by multiple several $\{a\}_m$.

A realistic case that may arise in subsurface modeling is that an indicator variogram along a vertical direction may be known from vertical well data, which provides the probabilities $\Pr(A_j=a_j|a_k)$ for any single k with the location k lying along the vertical of location j, see Figure 1. A training image may available in the horizontal direction from outcrop or shallow seismic surveys, from which one can obtain by scanning $\Pr(A_j=a_j|\{a\}_h)$ with $\{a\}_h$ being the set of all data lying in the same horizontal plane as location j, see Figure 1. All other values a neighboring location j will have to be ignored.

In a space-time context, one may have a 2D training image of the variable over geographical area and a 1D training image for time, providing two probabilities conditioned on two different data subsets.

Next, we need to consider the non-trivial challenge of combining all partial conditionals into one single conditional distribution model for A_j. The traditional kriging approach would call for the modeling of redundancy between any two data sets $\{a\}_k$ and $\{a\}_\ell$ in predicting A_j by means of their covariance. However, such modeling would be tedious for many reasons, first and foremost, there may not be any replicate of the pair of datasets $\{a\}_k$ and $\{a\}_\ell$ available that such modeling would call for.

In this paper, we therefore propose to avoid explicit modeling of data events redundancy by building that redundancy into the 3D spatial law itself. More precisely, we will employ Journel's *tau* model to combine partial conditionals into a full conditional. The *tau* parameters model the data redundancy of these subsets. The *tau* model can be written as follows

$$\Pr^*(A_j = a_j \mid a_{j-1},\ldots,a_1) = \Pr(A_j = a_j \mid \{a\}_1,\ldots,\{a\}_M) = \frac{1}{1+x} \text{ with}$$

$$\frac{x}{x_0} = \left(\frac{x_1}{x_0}\right)^{\tau_1}\left(\frac{x_2}{x_0}\right)^{\tau_2}\ldots\left(\frac{x_M}{x_0}\right)^{\tau_M} \quad \text{where:} \quad x_m = \frac{1-\Pr(A_j = a_j \mid \{a\}_m)}{\Pr(A_j = a_j \mid \{a\}_m)},\ x_0 = \frac{1-\Pr(A_j = a_j)}{\Pr(A_j = a_j)}$$

To understand the usefulness of this parametric redundancy model consider the same equation under log-form

$$\log x - \log x_0 = \sum_{m=1}^{M} \tau_m (\log x_m - \log x_o)$$

which is similar to the IK of (3). Consider the simple case where each

$$\{a\}_m = a_m, \quad m = 1,\ldots j-1$$

Knowing the indicator covariance means that all $Pr(A_j=a_j \mid \{a\}_m\} = Pr(A_j=a_j \mid a_i)$ are known, then solving the system (5) with Kriging would require knowledge of the spatial covariance.

In a full 3D multiple-point geostatistical approach, the inference of such redundancy is avoided since the full conditional can be directly read from the 3D training image, in other words, the training image itself is a redundancy model for the data $A_1 \ldots A_{j-1}$.

Another important property to consider is the closure of the *tau* model. This property states that if all information $A_1 \ldots A_{j-1}$ is used to predict A (no values are dropped) then the *tau* model is capable of modeling any probability distribution governing the unknown and the data. In other words, there exists a set of tau values for which one can combine the partial conditionals into a full conditional that will equal the full conditional directly inferred by considering all data $A_1,\ldots A_{j-1}$ jointly. In other words, any 3D spatial law can be reconstructed from lower dimensional information, if all information available is used and if the correct redundancy between the lower dimensional information is assessed. The latter is a non-trivial exercise because one would need 3D information to assess such redundancy, a case that is not considered in this paper.

Interpretation of the tau values

Before defining the particular algorithm for constructing 3D spatial models from partial spatial continuity information, it is instructive to review the interpretation of the tau values as provided by Krishnan (2004). Consider the case of two data sources $\{a\}_1$ and $\{a\}_2$ and set the $\tau_1=1$, hence

$$\frac{x}{x_0} = \frac{x_1}{x_0}\left(\frac{x_2}{x_0}\right)^{\tau} \qquad (6)$$

Then it is shown in Krishnan (2005) that $\tau = 1$ leads to

$$\frac{Pr(\{a\}_2 \mid A = 1 - a_j, \{a\}_1)}{Pr(\{a\}_2 \mid A = 1 - a_j)} = \frac{Pr(\{a\}_2 \mid A = a_j, \{a\}_1)}{Pr(\{a\}_2 \mid A = a_j)} = \text{constant}$$

One possibility to achieve this is

$$\Pr(\{a\}_2 \mid A = 1 - a_j, \{a\}_1) = \Pr(\{a\}_2 \mid A = 1 - a_j) \quad \text{and}$$
$$\Pr(\{a\}_2 \mid A = a_j, \{a\}_1) = \Pr(\{a\}_2 \mid A = a_j)$$

which means that datum $\{a\}_2$ is conditionally independent of datum $\{a\}_1$ given A_j.

$\tau > 1$ implies that the sensitivity of data set $\{a\}_2$ to a change in A_j is amplified by knowledge of dataset $\{a\}_1$, the larger τ, the larger that sensitivity. The reverse is true when $\tau < 1$. $\tau = 0$ means that dataset $\{a\}_2$ carries no information on A.

Sequential data redundancy

For given structural information and given redundancy parameters *tau*, the spatial model in (3a) is now fully defined. Simulating from such spatial law proceeds by sequential simulation as follows:

(1) A random location j is selected
(2) For that location, the partial information $\{a\}_m$, m=1,…,M from hard data and previously simulated nodes is gathered
(3) The partial conditionals $\Pr(A_j \mid \{a\}_m)$ m=1,…,M are calculated from the partial structural information
(4) The partial conditionals are combined with the *tau* model into a full conditional
(5) A simulated value is drawn
(6) Repeat (1) to (5) for all locations

This algorithm requires setting as many *tau* values as there are variables A_j to be simulated, which may be difficult as there are currently no methods available to determine these tau weights, nor do we have any data to do so. Note that in all rigor the tau values should be dependent on the unknown and the partial information. Instead of estimating the tau-values, the sequence of visits can be arranged such that a certain type of redundancy is expected, for example conditional independence (tau's=1). We will rely on the concept of sequential data redundancy to achieve this. Sequential data redundancy is a general concept referring to the sequential updating of information on an unknown by a series of ordered or ranked data sources. It lends itself particularly well to sequential simulation, where some variable A_j to be simulated depends on the sequence of previously simulated values. Values in this sequence can be grouped into one set (one data source), and given the structural information, some form of redundancy can be expected between these data sources. Consider the following example as illustration of this concept, see Figures 2 and 3.

Consider that we have a 2D training image as a model for the horizontal variability of the variable under study. Suppose this training image shows strong curvilinear, connected

highly non-Gaussian spatial patterns. In addition, a vertical variogram is available. The variable being simulated is a binary variable A(i,j,k) on a regular grid indexed by i,j and k.

To make use of sequential data redundancy, one simulates first all values that lie in the same plane using the 2D horizontal training image. Any plane k can be selected. This simulation would not call for any redundancy modeling, since a full 2D training image (2D redundancy model) is available. Next, one moves to another horizontal plane k′. The first node A(i,j,k′) visited in the second horizontal plane is simulated conditional to the value A(i,j,k) that lies in the previously horizontal plane, since no other conditioning information is available in plane k′. To maximally constrain the simulation of A(i,j,k) to the data in the previously simulated plane, the best choice for (i,j) would be to take the (i,j) location of the last simulated value in plane k, since this value is conditional to all previously simulated values in plane k. Hence in simulating A(i,j,k) an implicit conditional independence assumption is made

$$\Pr(A(i,j,k') \mid \{a(i,j,k)\}\ \forall i,j) = \Pr(A(i,j,k') \mid a(i,j,k))$$

Note that one cannot avoid making this assumption, due to the limited structural information available.

To simulate a second location (i′,j′,k′) in plane k′, one needs to condition to two data, the simulated values a(i′,j′,k) and a(i,j,k′). The horizontal training image is used to determine Pr(A(i′,j′,k′)=1| a(i,j,k′)), the indicator variogram is used to determine Pr(A(i′,j′,k′)=1| a(i′,j′,k)). The tau model is used to combine both into the joint conditional Pr(A(i′,j′,k′)=1| a(i′,j′,k), a(i,j,k′)). One can argue that setting both tau values to one is a plausible assumption in this case. Setting $\tau_1=\tau_2=1$ amounts to making the following assumptions

$$\begin{aligned} &\Pr(A(i',j',k) \mid A(i',j',k')=1, A(i,j,k')) = \Pr(A(i',j',k) \mid A(i',j',k')=1) \quad \text{and} \\ &\Pr(A(i',j',k) \mid A(i',j',k')=0, A(i,j,k')) = \Pr(A(i',j',k) \mid A(i',j',k')=0) \end{aligned} \tag{7}$$

In other words: information along the vertical screens information along the horizontal. (This does not mean information along the horizontal is not used (full independence), it just states some form of independence exists (tau's=1)). Suppose k′=k+1 or k′=k-1, then one can argue that this is a plausible assumption for this particular case, where more prominent spatial variability in the horizontal exist, compared to the vertical. To understand this better visually consider the situation in Figure 3 (a picture of 3D channel meandering). In case the true (unknown) 3D spatial variability is that of channel meandering, then knowing that a location along the vertical is inside/outside a channel makes information along the horizontal greatly (not fully) redundant, particularly if channel meandering is strongly sinuous. Eq (7) also motivates simulating the variable one horizontal plane after another, rather than the alternative which would be simulating along series of vertical lines. A conditional independence would not hold in such case since

$$\Pr(A(i',j',k) \mid A(i',j',k'), A(i,j,k') = 1) = \Pr(A(i',j',k) \mid A(i,j,k') = 1) \quad \text{and}$$
$$\Pr(A(i',j',k) \mid A(i',j',k'), A(i,j,k') = 0) = \Pr(A(i',j',k) \mid A(i,j,k') = 0))$$

would not be true for the situation in Figure 3 (channel meanders).

Examples

Case 1: horizontal XY training image (250x250), Figure 4, and 2D vertical YZ variogram. Consider the case where a horizontal training image is available as well as a variogram model describing variability in a cross-section. This cross-section is orthogonal to the channel meanders. The variogram is isotropic spherical with a range of 10 units. The range is taken the same as the channel width. A 3D model will be constructed by successively generating horizontal slices.

Figure 5A shows the first horizontal slice generated using the 2D horizontal training image. Figure 5B shows the map of conditional probabilities $\Pr(A(i,j,2)=1|\{a(i,j,1)\ \forall i\})$, i.e. the conditional probability of A(i,j,2), given information from the previously simulated horizontal plane. However, since in the vertical direction only the variogram in a 2D YZ section is available, only values a(i,j,2) with the same j-index can be retained to derive such vertical conditional probabilities. These vertical conditional are combined with the horizontal conditional $\Pr(A(i,j,2)=1|\{a(i,j,2)\ \forall i,j$ previously simulated$\})$ to form the full conditional from which a values is simulated. In case one would have chosen a range of 2 (less vertical correlation), the map of vertical probabilities in Figure 5C would have been obtained. Figure 5C shows more uncertainty (due to lesser correlation) than Figure 5B.

The full 3D model of dimension 50x100x50 is shown in Figure 6 for various tau values (Eq. (7) is used where x_2 related to the vertical variogram information). For each 3D model a 2D YZ variogram was calculated of which the Y and Z-directions are shown in Figure 7. Figure 8 shows the case when tau=1.2. In the latter case, the variogram is well reproduced. Variogram reproduction could be used a criterion to set the tau-value.

Case 2: horizontal XY training image (250x250), Figure 4, and 1D vertical Z-variogram. In this case we consider that only a 1D variogram is available. Several values of tau were tried, the results gathered in Figure 9. Again, we find that a value of tau close to 1 provides a satisfactory variogram reproduction.

Case 3: Figure 10 shows the case where the XY continuity is provided by a complex system of braided channels, while the YZ plane continuity is simply a stacking of such channel bodies as represented by a vertical 2D training image generated with GSLIB program *ellipsim*. Using a parameter tau=1 the results in Figure 11 are obtained showing good reproduction of the braiding as well as stacking of the channels in 3D.

Case 4: Another useful application of this method lies in the reproduction of 3D pore space from 2D cross-section. The reconstruction of 3D pore space from 2D thin section

photos is useful in many applications of multiphase flow through porous media, such as in the determination of reservoir permeability and relative permeability, studying the behavior of capillary pressure as function of saturation (Blunt et al, 2002, Chen and Doolen, 1998). A paper by Okabe and Blunt (2005) presents a multiple-point geostatistical method for generating such 3D pore space from 2D section, relying on a much simpler model than the tau-model. In fact they use a simple weighted average of the various partial conditional distributions. While this has some evident theoretical limitations (no compounding possible), the resulting models seemed to reproduce well the statistical information from each section.

The data used for this study consists of a micro CT scanning of the Fontainebleau sandstone, see Figure 12. From this 3D reference model an XY and YZ section was extracted, to be used as input to our method.

First, a standard variogram approach was used, whereby first the variogram in several directions was calculated. As seen in Figure 13, the variogram is basically isotropic with a range of 8 cells. An assumption of isotropy was then made fro the 3D variogram. This 3D variogram is used in S-GEMS program *sisim* to simulate in 3D the pore space, see Figure 14. The proportion (porosity) was taken the same as the reference (=22%).

Next, the above proposed method is used to simulate the 3D pore space, with tau=0.8 by (1) simulating consecutive horizontal slices, see Figure 15, (2) consecutive vertical slices, see Figure 16. At least visually the results are very similar: this is to be expected since the medium appears fairly isotropic, i.e. the patterns in both training images are similar. However, compared to the *sisim* model, it appears visually that the narrow pore throat pattern is much better reproduced. Future work will investigate what the difference in permeability and other flow-related properties between the multi-point and two-point models are.

Conclusions

Building 3D models using a geostatistical estimation or simulation method calls for a full 3D model of spatial continuity, whether implicit or explicitly stated. A 3D training provides one way to explicitly disclose 3D spatial information. However, in many practical cases, 3D spatial continuity may not be immediately or explicitly available, hence models are required to combine all spatial continuity information, typically of lower dimension (1D or 2D) into a full 3D model. This paper provides a method for combining lower dimensional information into a full 3D model. This 3D model can then be used as training image for further stochastic simulation and data integration. Further application and extensions to non-binary problems will need to be investigated to explore the limits of applicability and gain more insight into when this method can be used.

References

Blunt, M.J., et al. 2002. Detailed physics, predictive capabilities and macroscopic consequences for pore-network models of multi-phase flow. Advances in Water Resources 25, 1069-1089.

Chen, S and Doolen, G.D., 1998. Lattice Boltzmann method for fluid flows. Ann. Rev of Fluid Mechanics, 30, 329-364.

Journel, A. G.: "Combining Knowledge from Diverse Sources: an Alternative to Traditional Data Independence Hypothesis," Mathematical Geology, Vol. 34, Iss. 5, July 2002.

Krishnan, S.: The Tau Model to Integrate Prior Probabilities, Ph.D. Dissertation, Stanford University, December 2004.

Okabe, H. and Blunt, M.J., 2005. Pore space reconstruction using multiple-point geostatistics. Journal of Petroleum Science and Engineering, 46, 121-137.

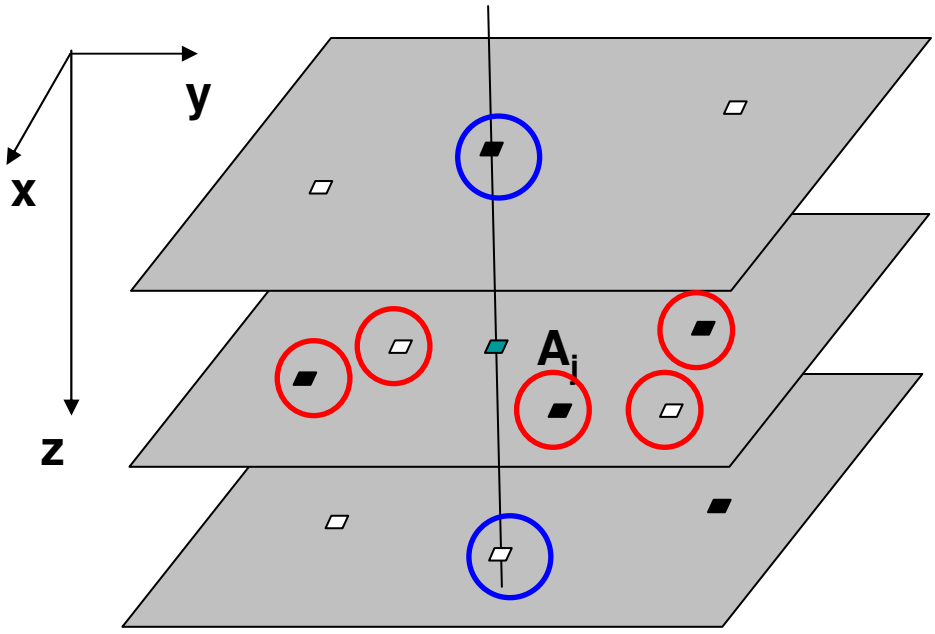

$\{a\}_v$ = 2 vertical data

$\{a\}_h$ = 5 horizontal data

Other data must be ignored

Figure 1: In case only partial information is available then some data must be ignored

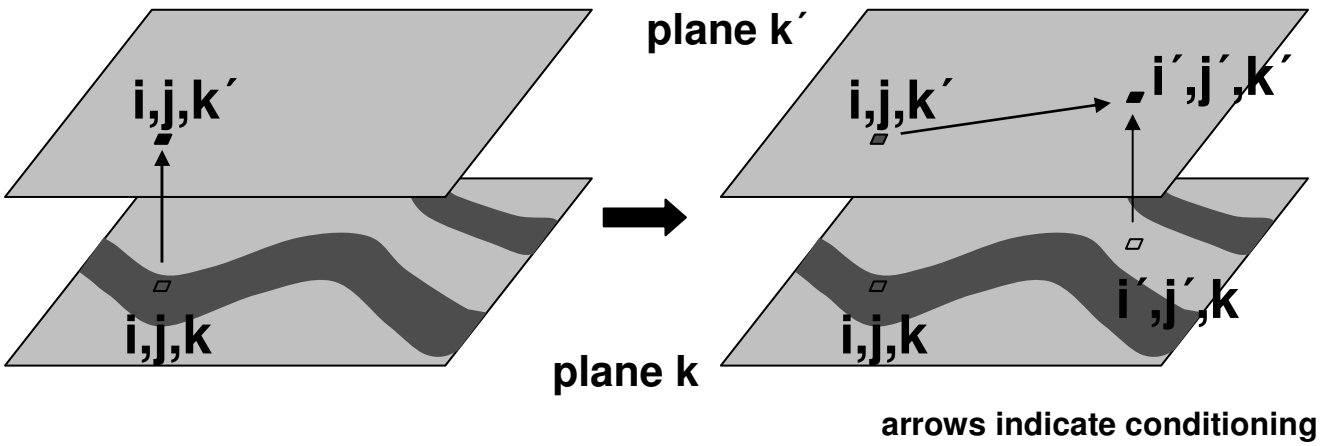

Figure 2: sequential conditioning: plane k is simulated before plane k'

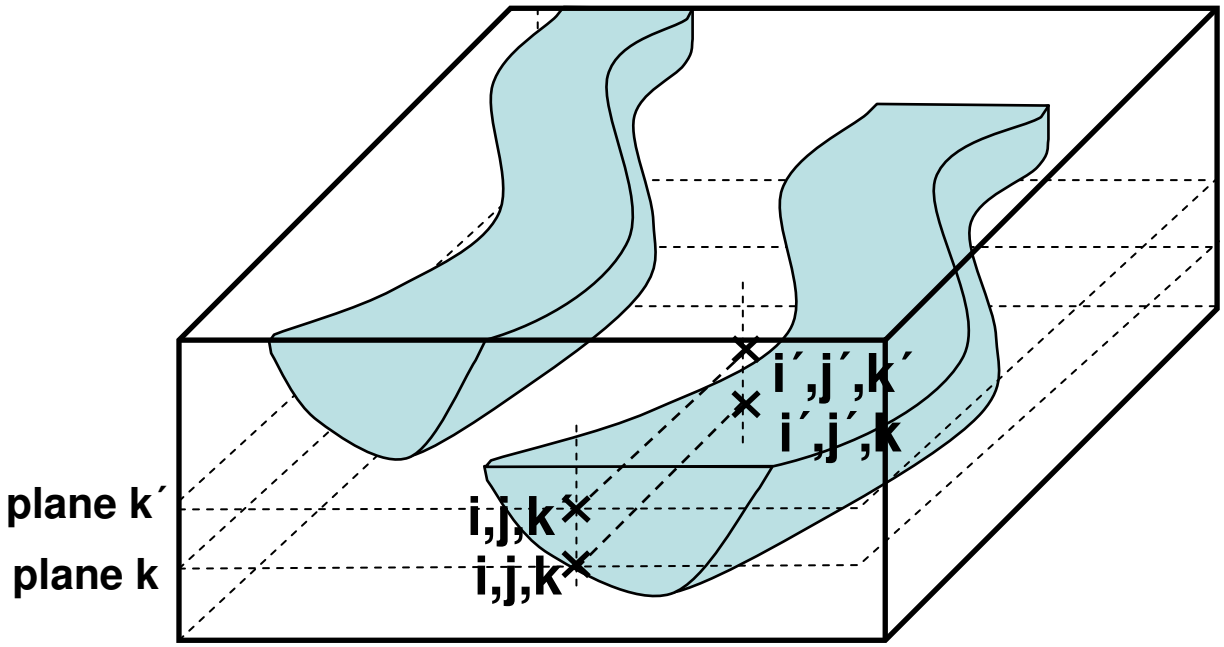

Figure 3: conditional independence can be reasonably assumed since the horizontal variability is less predictable than the vertical one.

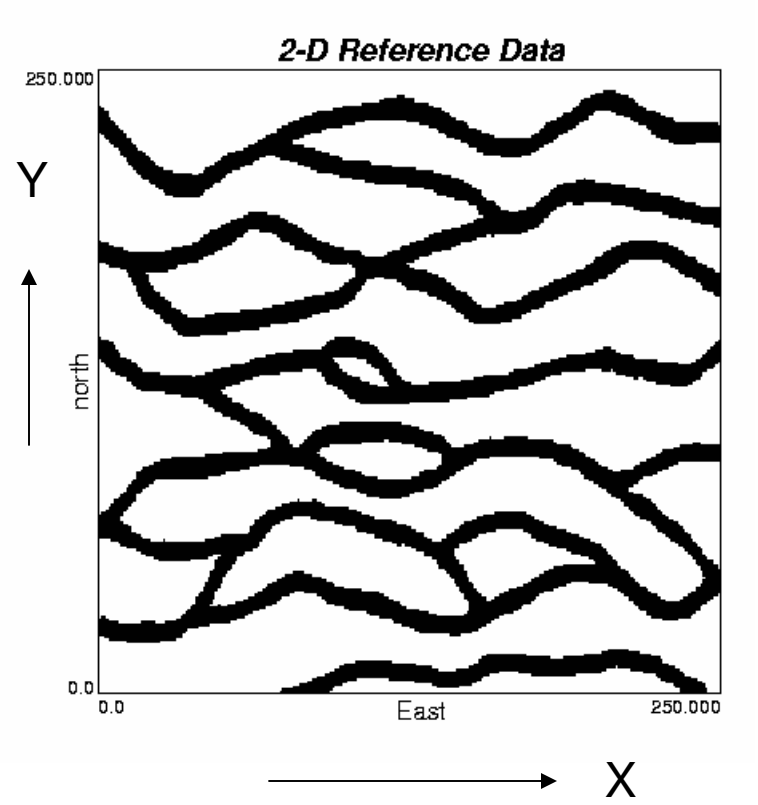

Figure 4: In case only partial information is available then some data must be ignored

A

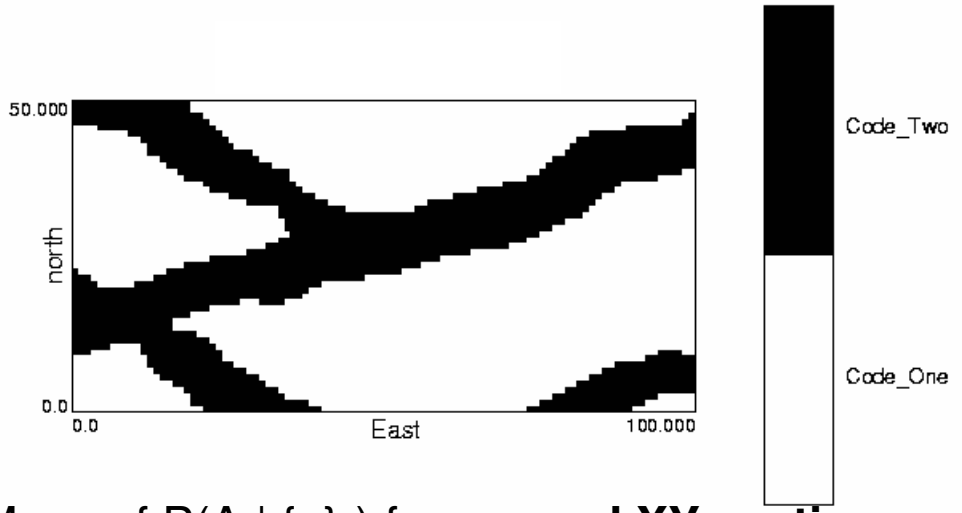

Maps of P(A | $\{a\}_v$) for **second XY section**

$\{a\}_v$ is the vertical data from first slice

B

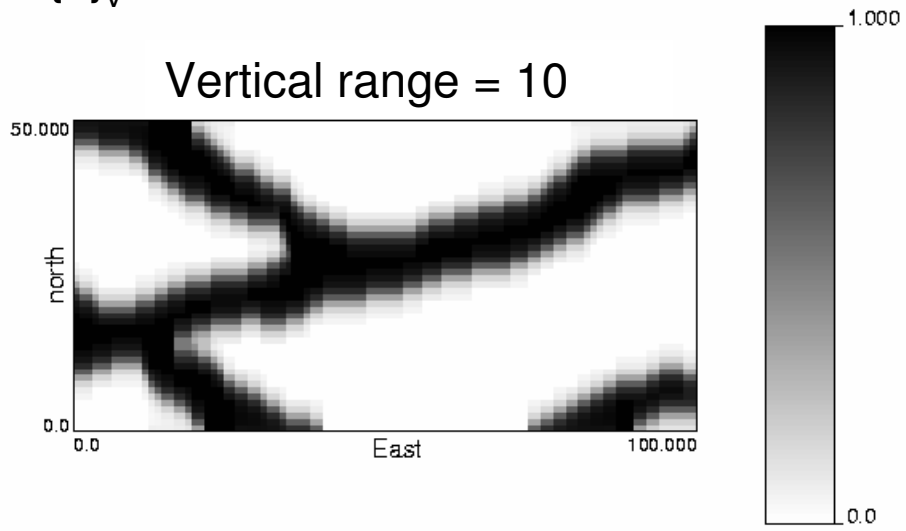

C

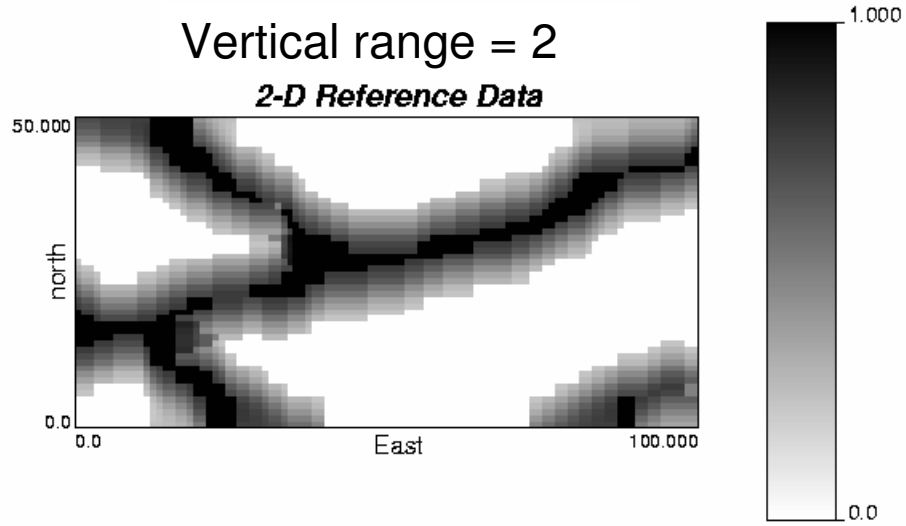

Figure 5: (A) first horizontal slice of 3D model (B) conditional probabilities related to the variogram, range=10, (C) case of range=2

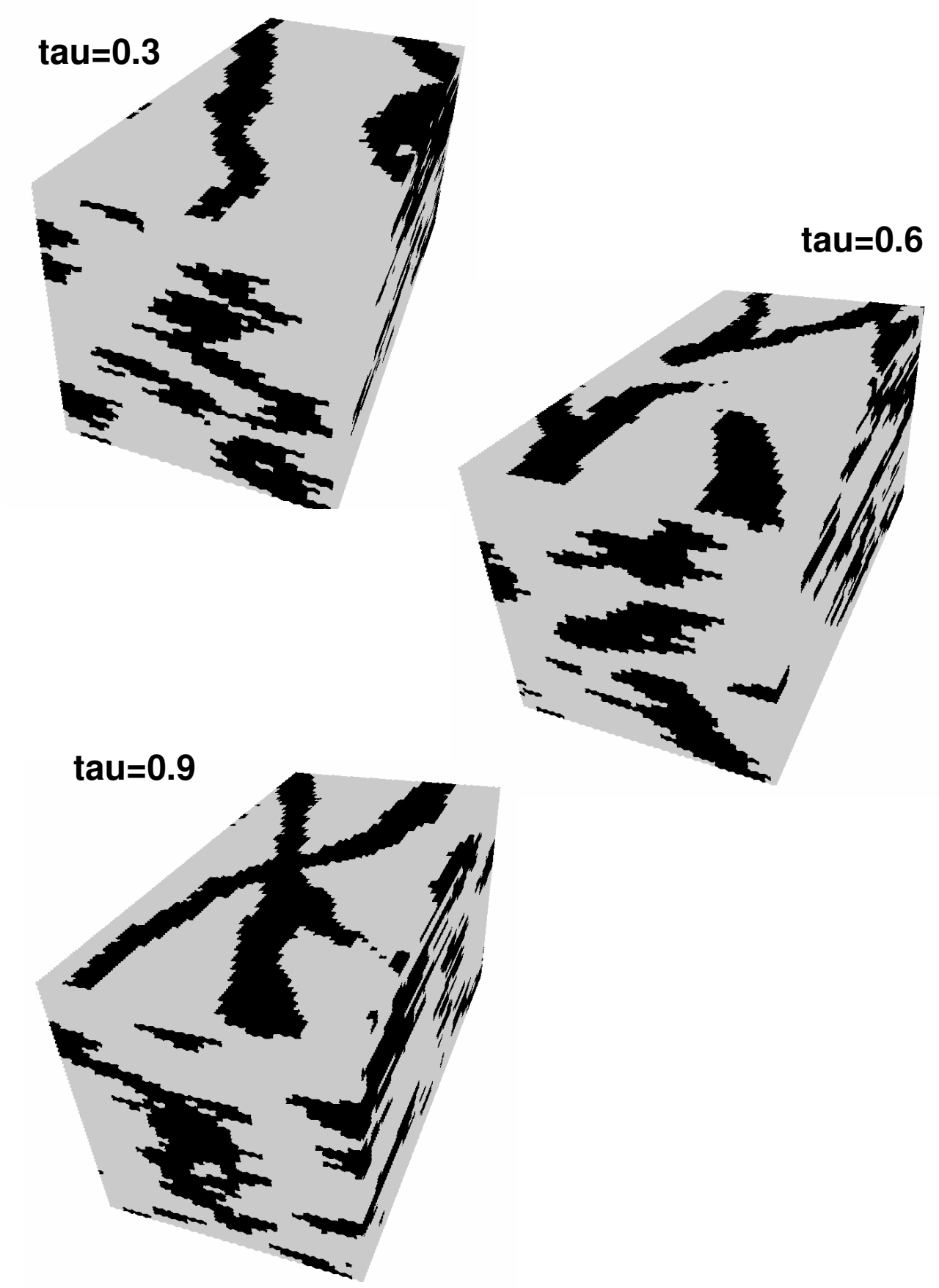

Figure 6: 3D models built for various values of tau

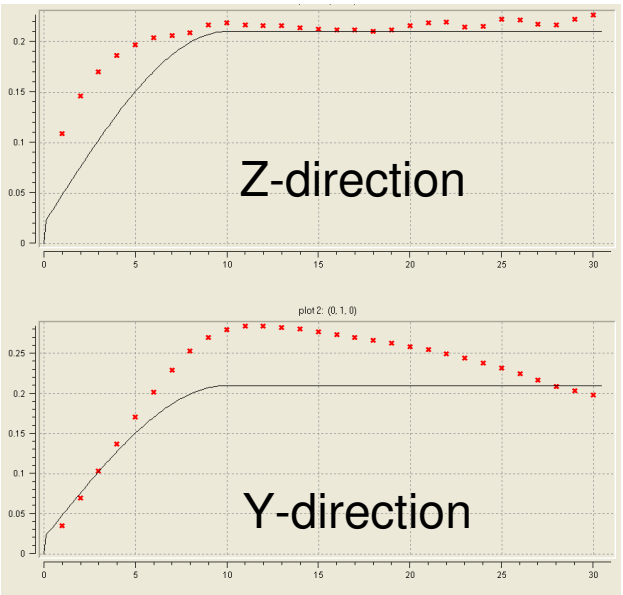

tau=0.3

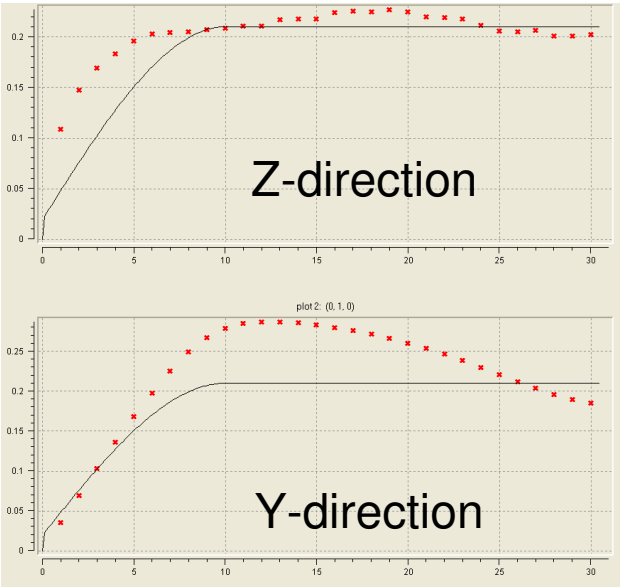

tau=0.6

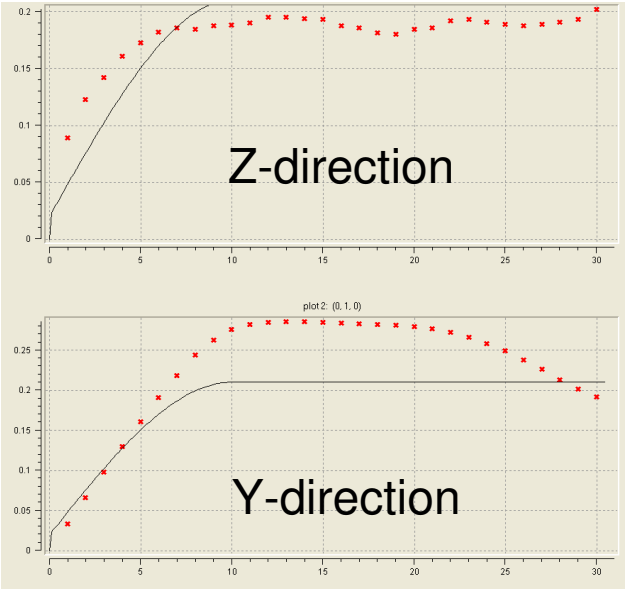

tau=0.9

Figure 7: variogram of models

In Figure 6

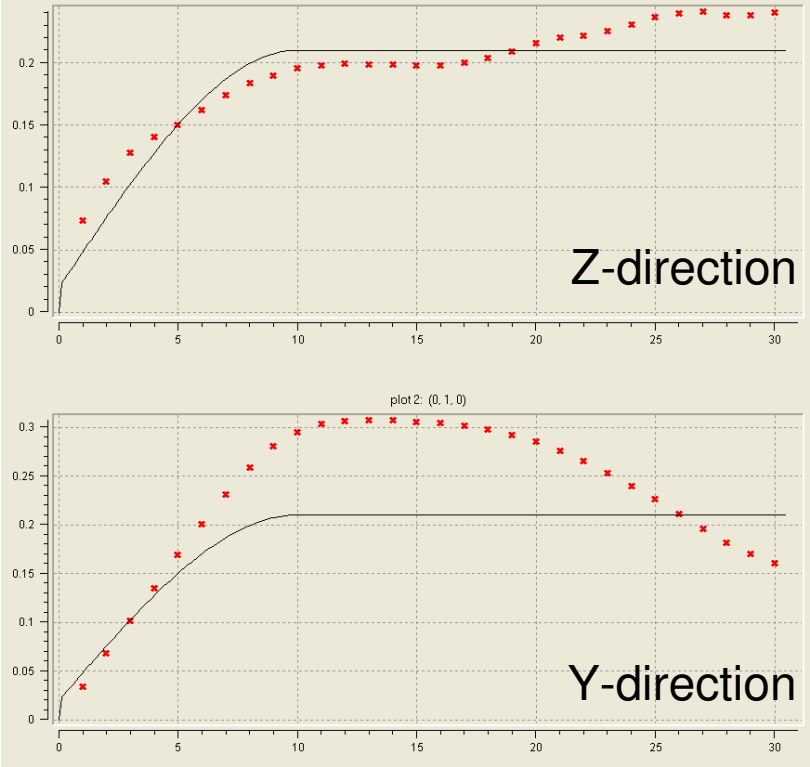

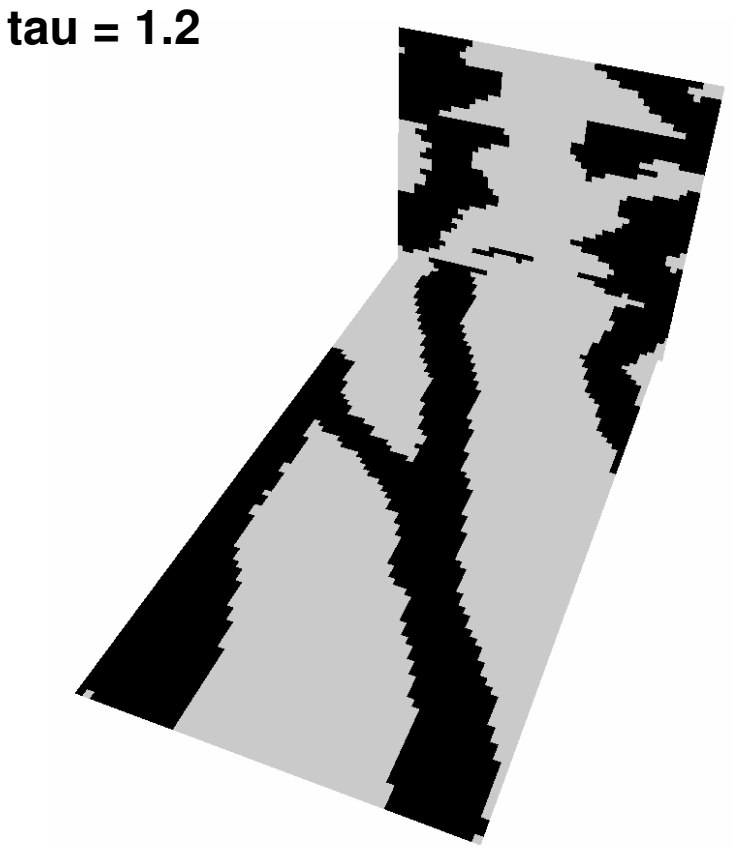

Figure 8: Case with tau=1.2

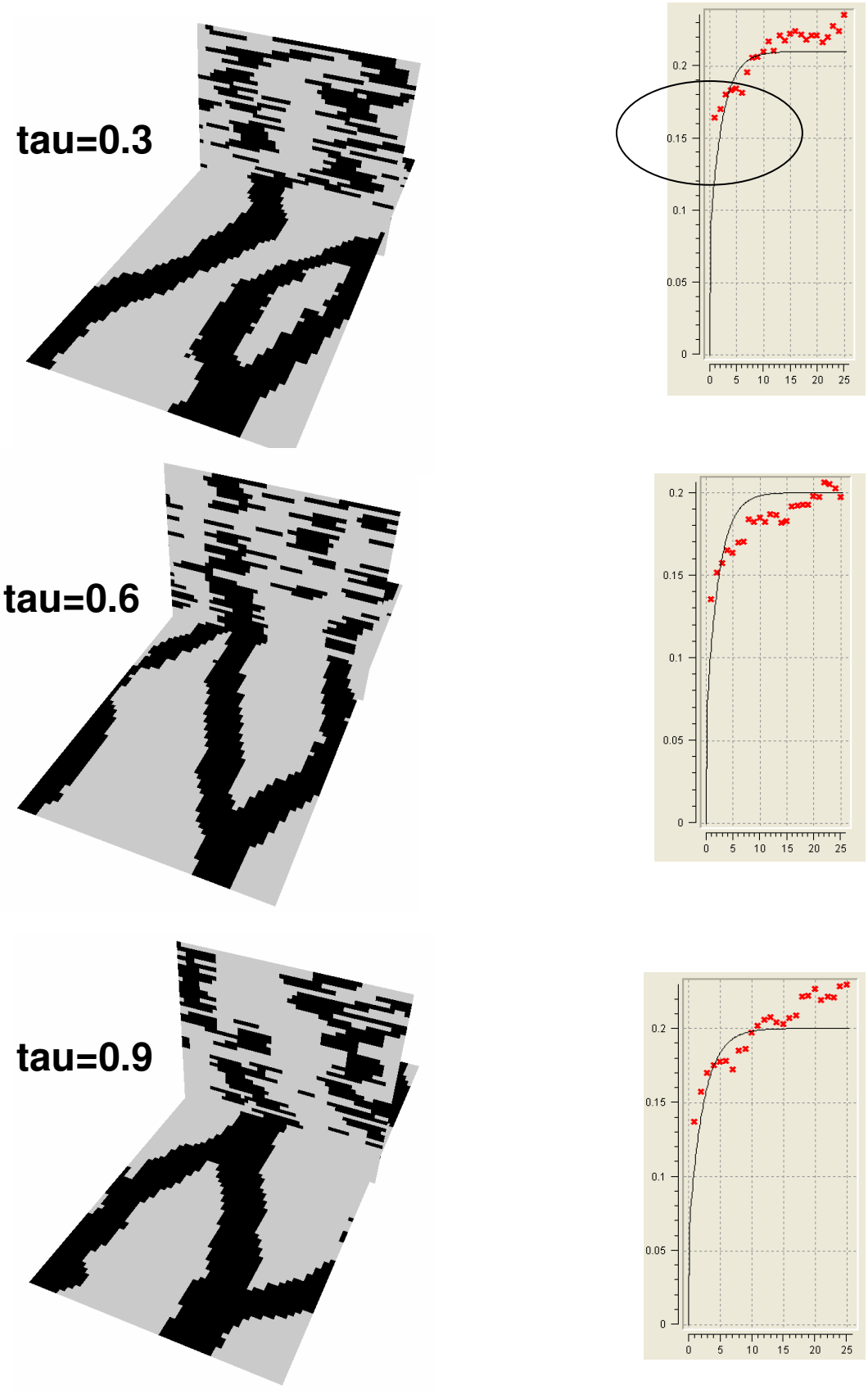

Figure 9: Case 2, with 1D vertical variogram only, several tau-values

Horizontal TI 1000 x 400

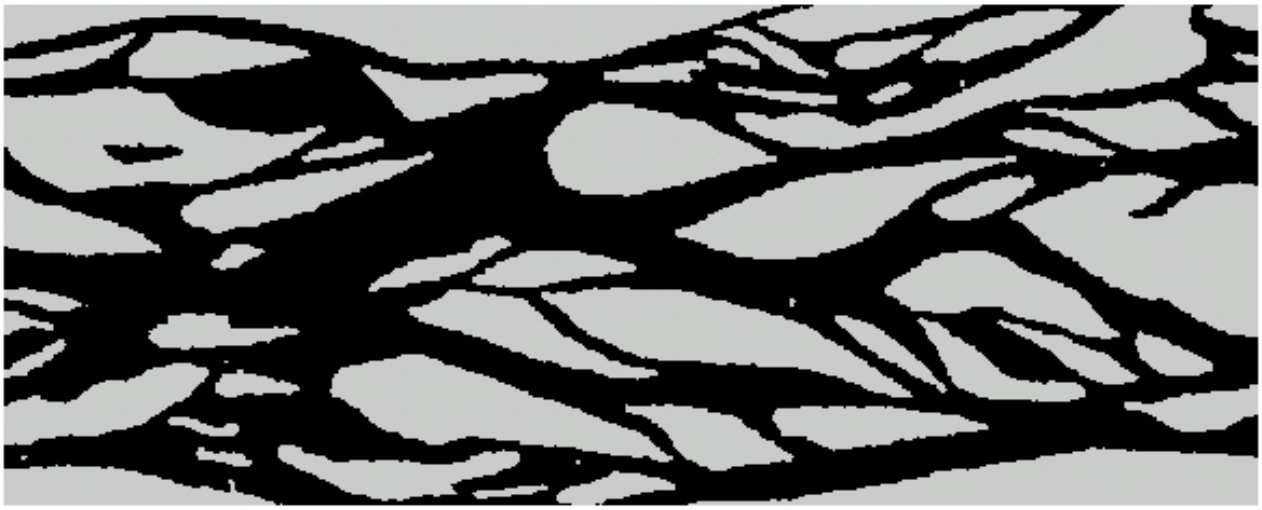

Braided system in New Zealand (from Ph. Renard)

Vertical TI 400 x 100

generated with ellipsim

Figure 10: XY continuity provided by braided river system, YZ continuity generated by ellipsim representing stacking of channel bodies

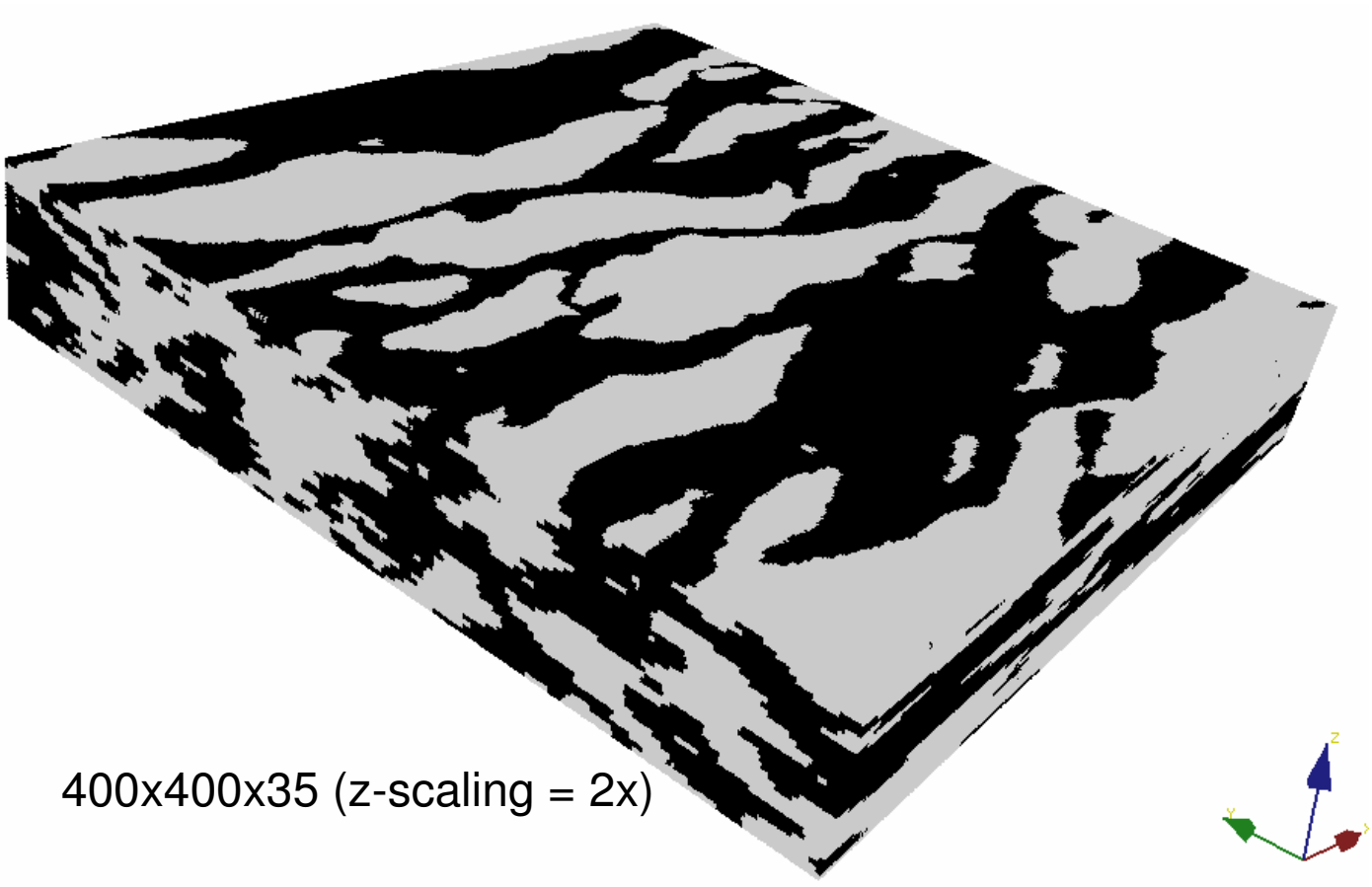

YZ sections

XY sections

Figure 11: Single 3D model

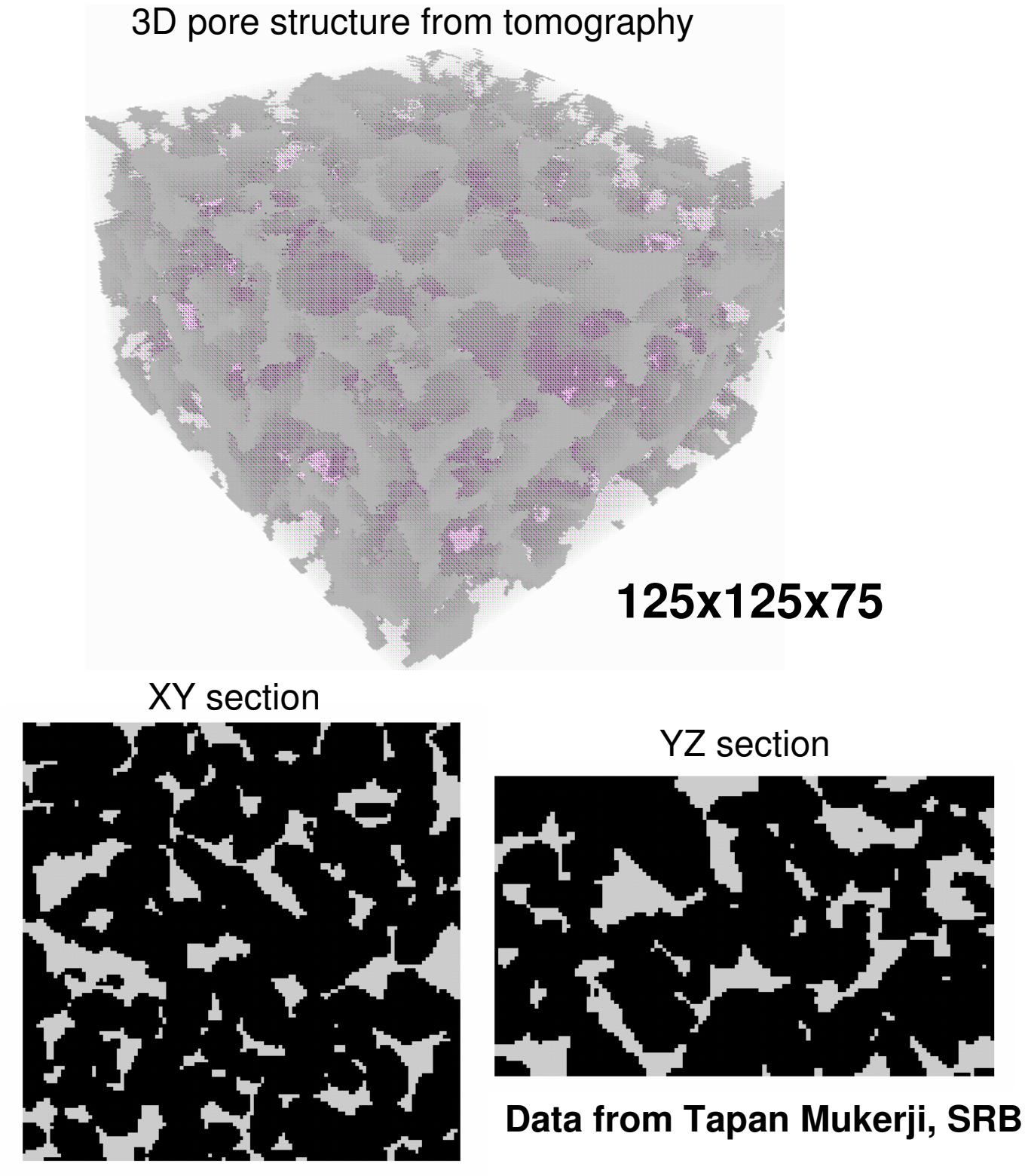

Figure 12: Fontainebleau sandstone cross sections and 3D view of pore space

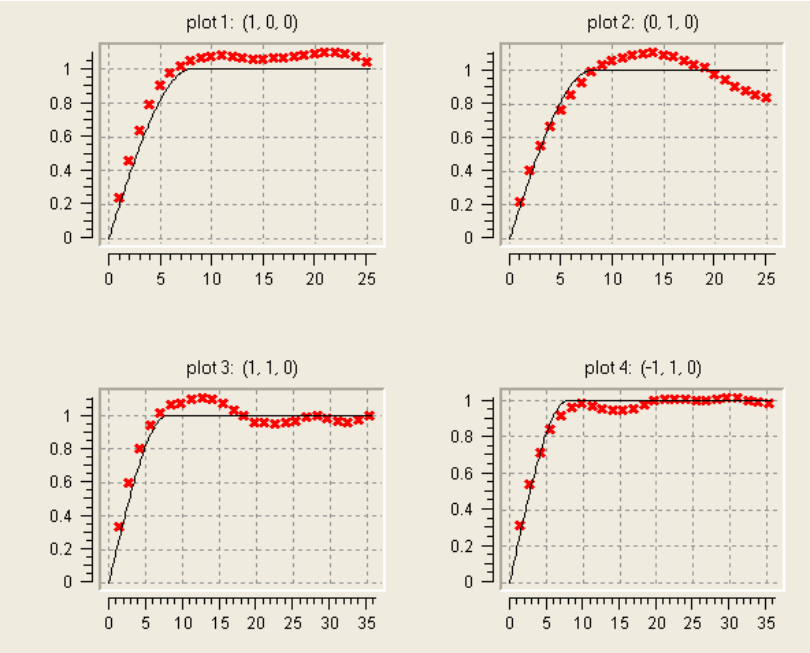

Horizontal section

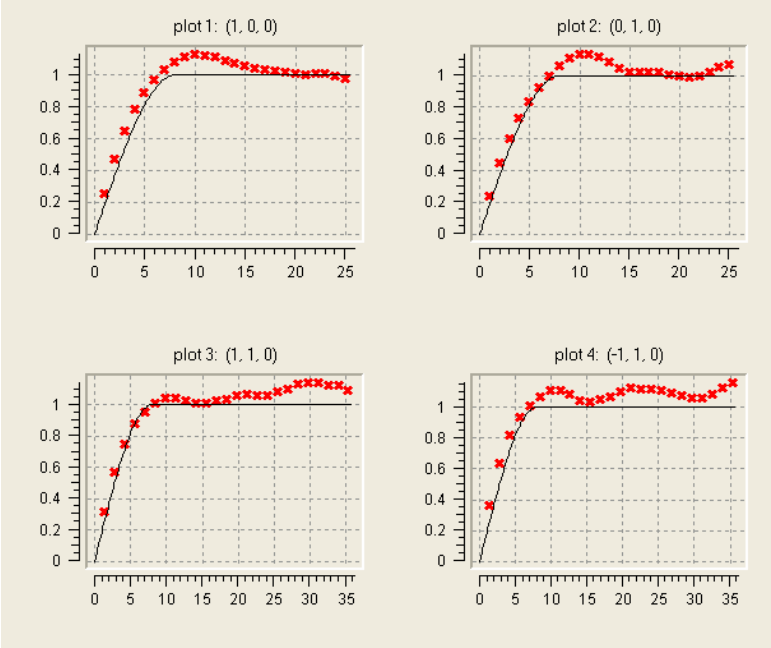

Vertical section

Figure 13: Variograms calculated over several directions in each section

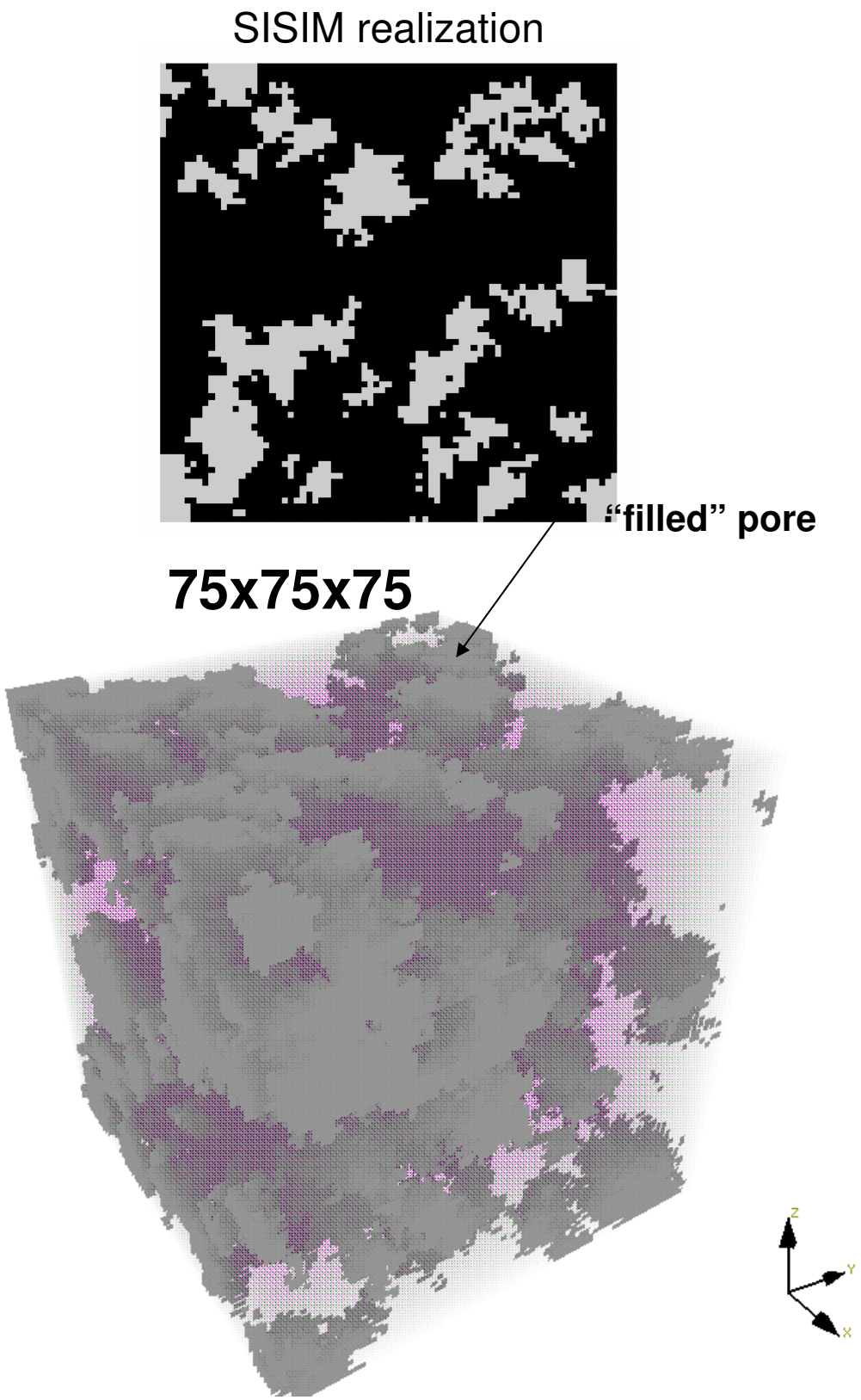

Figure 14: sisim simulation of the 3D pore space

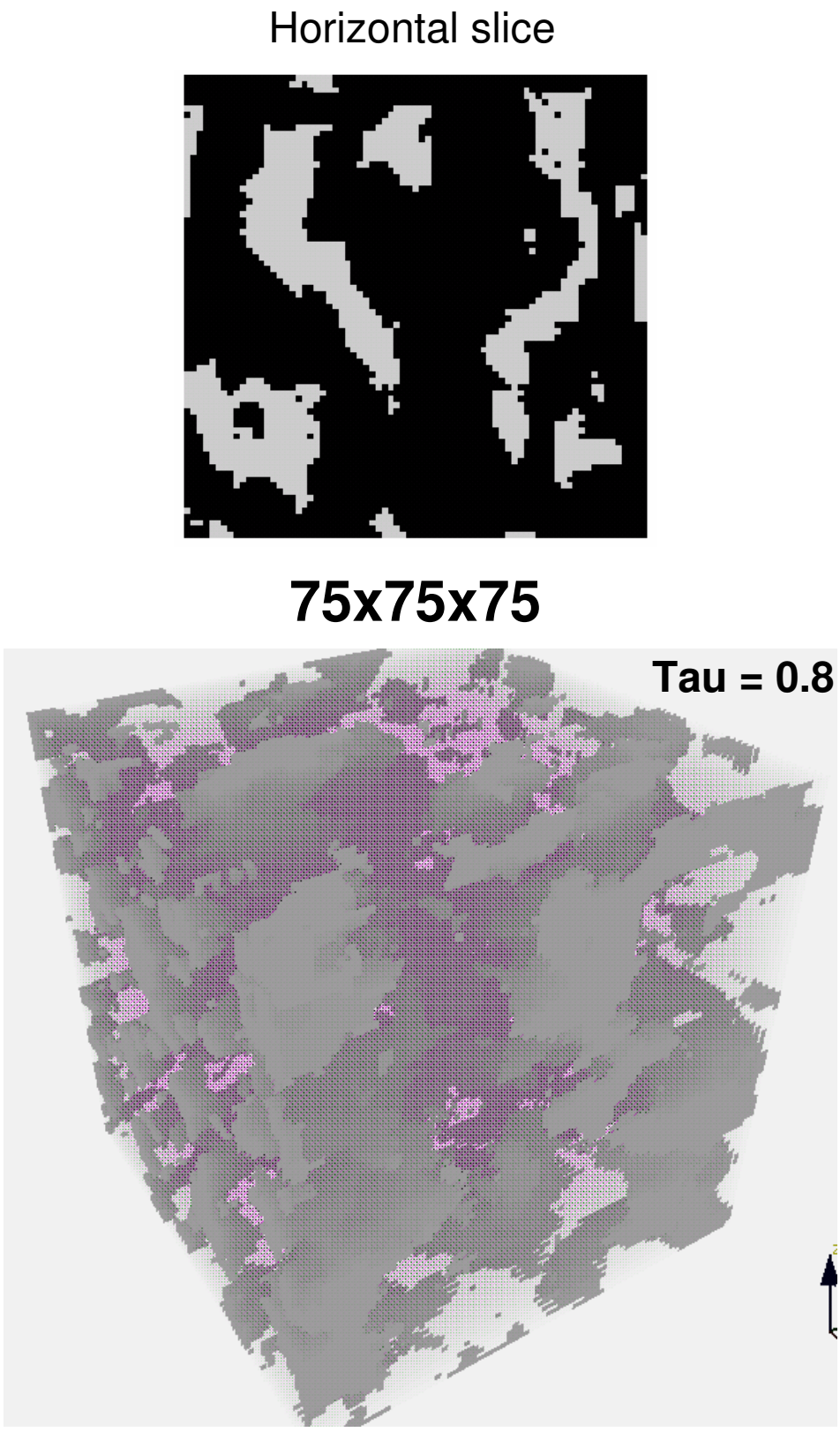

Figure 15: simulation of the 3D pore space using mp-statistics, simulation of stacked horizontal slices

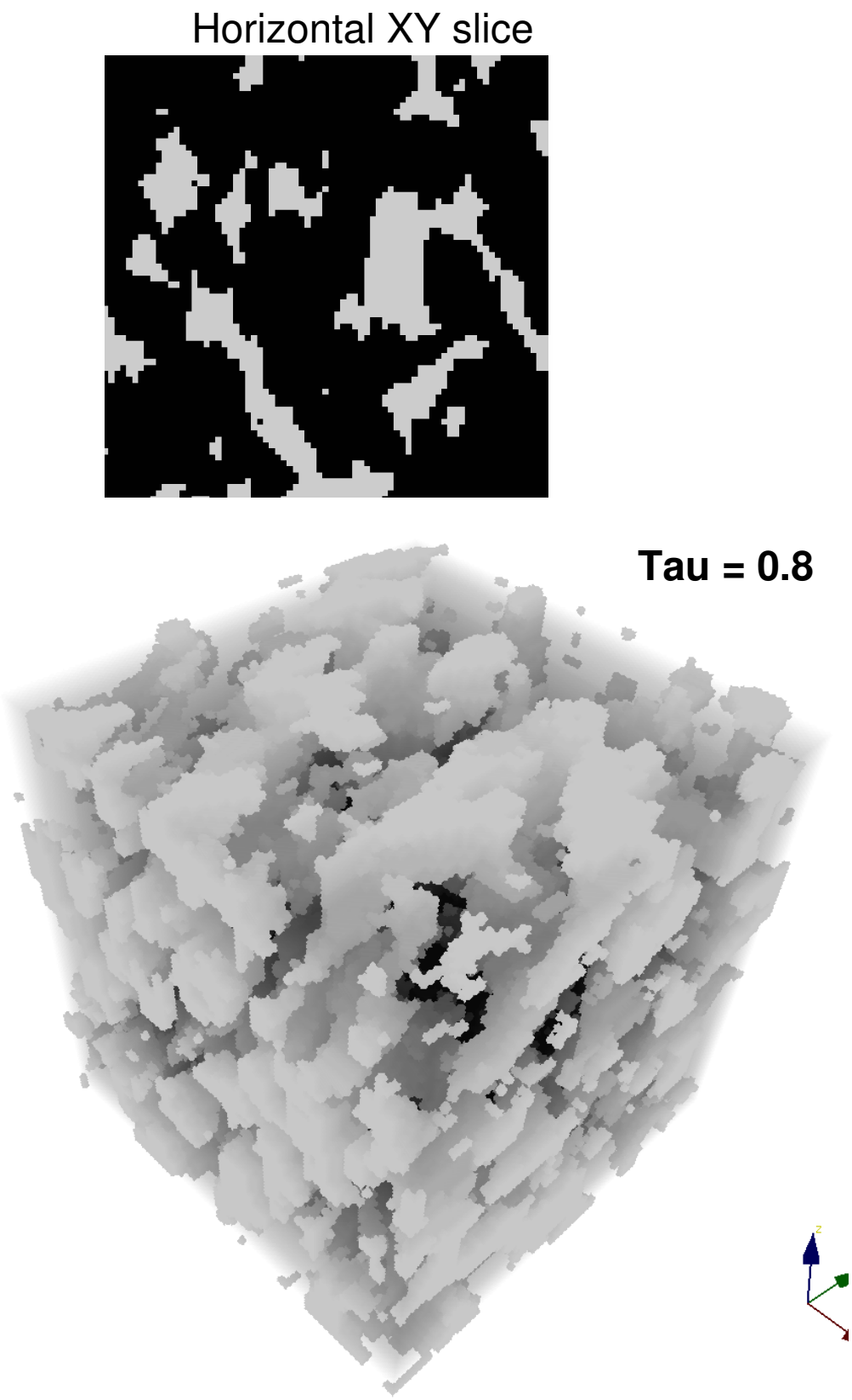

Figure 16: simulation of the 3D pore space using mp-statistics, simulation of tiled vertical slices